Ceramics-Silikáty 67 (3), 282-290 (2023)
www.ceramics-silikaty.cz doi: 10.13168/cs.2023.0028

MONITORING THE INTERACTION OF SYNTHETIC HYDROXYAPATITES UNDER VARIED IN VITRO TEST CONDITIONS

#DIANA HORKAVCOVÁ*, MARGAUX GUIRAUD**, GISÉLE LAURE LECOMTE-NANA**, MILOSLAV LHOTKA***, ALEŠ HELEBRANT*

*Department of Glass and Ceramics, Faculty of Chemical Technology, University of Chemistry and Technology Prague, Technická 5, 16628 Prague, Czech Republic
**Institut de Recherche sur les Céramiques, ENSIL-ENSCI, 12 rue Atlantis, Université de Limoges, 87068 Limoges, France
***Department of Inorganic Technology, Faculty of Chemical Technology, University of Chemistry and Technology Prague, Technická 5, 16628 Prague, Czech Republic

#E-mail: diana.horkavcova@vscht.cz

Submitted June 20, 2023; accepted July 26, 2023

Keywords: Hydroxyapatite, Simulated Body Fluid, Tris, In vitro

The experimental work focuses on the detailed monitoring of the interaction of commercial hydroxyapatite (HA) granules with various morphologies and surfaces with simulated body fluid (SBF) under varied in vitro test conditions. The ISO 23317:2014 standard, which specifies methods for the detection of apatite formation on the surface of materials in a simulated body fluid, mainly focuses on one-piece samples (tablets, rectangular shaped samples) under static conditions. The SBF solution modelling the inorganic part of blood plasma is buffered with a Tris buffer which can, under certain conditions, affect the in vitro test results by its own interaction with the tested material. Changes on the surfaces of the tested bioceramic granules with varied porosity and leachates from the buffered and unbuffered SBF solutions were characterised at selected time intervals using the available methods (SEM, BET, AAS, UV-VIS). The kinetics of the formation and morphology of the precipitated hydroxyapatite (HAp) was found to vary under different in vitro test conditions. The leachates from the solutions confirmed different rates of calcium and phosphate ions depletion, especially at the beginning of the assay. The pH analyses of the buffered and unbuffered SBF solutions also showed a Tris buffer effect.

INTRODUCTION

Synthetic hydroxyapatite (HA, $Ca_{10}(PO_4)_6(OH)_2$) is one of the most widely used ceramic biomaterials in the field of reconstructive medicine because its chemical composition is the closest to the inorganic component of bones [1]. In relation to its interaction with the living organism, it is classified as a bioactive material because it is chemically (through a precipitated layer of the bone-like hydroxyapatite) fixed to the hard tissue [2]. Hydroxyapatite, in the form of powders, granules or scaffolds, is produced by several methods, e.g., by precipitation from calcium-phosphate solutions or by the sol-gel method [3-10]. Great efforts have been made to produce hydroxyapatite from natural materials (such as animal bones, shells, eggshells, etc.) in order to make its properties as similar as possible to natural apatite [11-14]. Much attention has been paid to the use of hydroxyapatite in the form of porous granules and scaffolds for pharmaceutical applications (antiresorptive drugs, anticancer drugs, gene therapy, proteins, antibiotics and others) [15]. In order to prevent bacterial colonisation and to reduce infections, dopants, such as silver, zinc, copper or strontium, are incorporated into synthetic hydroxyapatite, which may improve the existing properties of the bioceramic material [16]. The hydroxyapatite enriched in this way acquires antibacterial properties, which are currently essential in the field of medicine [16, 17]. The antibacterial effect is most frequently tested against the bacterial strains of *Escherichia coli*, *Staphylococcus aureus* or the yeast *Candida albicans* [16-18]. In recent years, biomaterials have also been monitored against cell lines [19]. Testing of bioactive properties is performed *in vivo* in live laboratory animals [20] or *in vitro* in simulated body fluids (SBFs) [21-23]. The *in vitro* tests serve mainly as a prediction of the behaviour of synthetic materials by exposure in a physiological solution mimicking the inorganic part of blood plasma. ISO 23317:2014(E) is used to investigate the ability of materials to form an apatite layer on their surface [24]. Precipitation of the layer is an indicator of the bioactive behaviour of the tested material. The standard recommends testing materials in the form of tablets or plates, while maintaining the relationship

V_S = 100 mm.Sa (V_S is the volume of the SBF in mm^3, S_a is the apparent surface area of the specimen in mm^2). The standard does not precisely define the testing conditions for highly macro- and micro-porous materials or granules that can be used as fillers. The standard only provides the following recommendation: For porous materials, the volume of the SBF should be greater than the calculated one [24]. Some in vitro tests that monitored the bioactivity (in order to better approximate the conditions in a living organism) were performed under semi-dynamic conditions, where the SBF solution was exchanged for a fresh one at certain intervals [25], or under dynamic conditions, where the solution was circulated using a peristaltic pump [26]. It is known from our previous scientific works that the type of material, its specific surface area, porosity, pore size and volume filling rate are very important parameters for *in vitro* testing. A question was asked whether the static conditions lasting for several weeks, as presented in the standard, are suitable for testing of highly bioactive granular and highly porous materials. The experiments also raised the question about the involvement of the Tris buffer, which is used to maintain the pH of the simulated body fluid, in the actual interaction with the tested material [27-30].

This work monitors effects of the SBF solution volume (V_1, V_2) and the Tris buffer on two types of hydroxyapatite synthetic materials. The experimental work is related to other papers [27, 28] which addressed the filling rate of the bioceramics space/volume (1V and 1/4V) and the effect of the chemical composition of the biomaterials (TCP and HA) on the bioactive behaviour under dynamic *in vitro* assay conditions. The setting of the *in vitro* assay conditions is very important for other than one-piece samples [29], as the standard is defined for one-piece samples. Another important parameter is the analysis of the changes in the ion concentrations in the leachates. The results of one work [30] indicate an important effect of the buffer on the stability of the solution. Testing is important because it can serve as a prediction in the development of new fragmented bioceramic materials (granules, particles, crushed material) used in medical structural regenerative applications.

EXPERIMENTAL

Tested materials and conditions of *in vitro* test

Two bioceramic materials based on pure hydroxyapatite (HA, $Ca_{10}(PO_4)_6(OH)_2$) synthetic and commercially available powders with different morphologies and surfaces were used for the in vitro tests with two volumes (V_1; V_2). Sintered granules sized 1-3 mm with a specific weight of 2950 - 3140 $kg \cdot m^{-3}$ and tensile strength of 40 - 60 MPa, and micro- and macro-porous granules sized 1 - 2 mm with a porosity in the range 60 - 70 % interacted with two types of simulated body fluid (SBF) which represented the inorganic part of the blood plasma (Table 1). The SBF solutions were prepared by the gradual dissolution of NaCl, $NaHCO_3$, KCl, $KHPO_4 \cdot 3H_2O$, $MgCl_2 \cdot 6H_2O$, HCl, $CaCl_2$ and Na_2SO_4, according to the standard [24]. The first solution was buffered with the Tris buffer (Tris-hydroxymethyl aminomethane) and HCl (**SBF**+**T**), while the second solution was buffer-free (**SBF** only).

Table 1. Composition of the simulated body fluid (SBF) and blood plasma (BP) [24].

solution	Ionic concentration ($mmol \cdot l^{-1}$)							
	Na^+	K^+	Ca^{2+}	Mg^{2+}	Cl^-	HCO_3^-	HPO_4^{2-}	SO_4^{2-}
SBF	142.0	5.0	2.5	1.5	147.8	4.2	1.0	0.5
BP	142.0	5.0	2.5	1.5	103.0	27.0	1.0	0.5

Granules of commercial hydroxyapatite with low and high specific surface areas (**HA-L**, **HA-H**), weighing 0.05 ± 0.001 g, interacted with the two types of solution (**SBF+T**, **SBF**), with the volumes of V_1 = 50 ml and V_2 = 100 ml. The types of the material and solutions, the volumes and sample identifications are shown in Table 2. The static in vitro assay was performed for 21 days. The temperature of both types of solution was maintained at 36.5 °C using a thermostat. The materials were analysed and changes in the pH values and calcium $(Ca)^{2+}$ and $(PO_4)^{3-}$ ion concentrations were monitored in the leachates at selected intervals (0, 7, 14 and 21 days).

Table 2. Conditions of the *in vitro* test.

Material	Surface	Type of solution	Volume (ml)	Title
Hydroxyapatite	Low	SBF	50	HA-L/SBF/50
			100	HA-L/SBF/100
		SBF+T	50	HA-L/SBF+T/50
			100	HA-L/SBF+T/100
	High	SBF	50	HA-H/SBF/50
			100	HA-H/SBF/100
		SBF+T	50	HA-H/SBF+T/50
			100	HA-H/SBF+T/100

Methods for the characterisation of the materials and solutions

The surfaces of the ceramic biomaterials before and after the interaction were observed using a Hitachi S-4700 electron microscope with a Thomson Scientific Ultradry Silicon Drift Detector energy dispersive analyser (EDS) at an accelerating voltage of 15 kV and an emission current of 20 μA. The non-conductive samples were coated with an Au-Pd layer.

The specific surface areas of the materials before and after the interaction were determined by the Brunauer–Emmett–Teller (BET) method using the ASAP 2020 V3.00 H instrument made by Micromeritic, using N_2 gas. The concentration of the calcium ions in both types of leachates was analysed by atomic absorption spectrometry using an Agilent 280FS AA. Atomisation was carried out with an acetylene-N_2O flame. The wavelength of 422.7 nm was used for the absorbance measurements. The concentration of the phosphate ions was analysed on a UV-VIS spectrophotometer UV1601 at λ = 830 nm according to EN ISO 6878. The pH value was measured with an inoLab pH-meter with a combined glass electrode at 36.5 °C.

RESULTS AND DISCUSSION

Specific surface characterisation

The values of the specific surface area (S_a) of the two types of synthetic hydroxyapatite before (0 day) and after 7, 14 and 21 days of interaction with the two volumes of **SBF** and **SBF+T** solutions are shown in Table 3.

The first obtained data clearly indicated that changes of the specific surface area are the most dramatic during the first 7 days of interaction with the solutions. The value for the sintered material changed from 0.6 to 1.4 - 2.5 $m^2 \cdot g^{-1}$ and it changed from 49.4 to ca 61.5 $m^2 \cdot g^{-1}$ for the porous material. The changes to the specific surface area values between 7 and 14 days of exposure were very small for the porous hydroxyapatite (HA-H/SBF/50; HA-H/SBF/100; HA-H/SBF+T/50). The most reactive material was the sintered hydroxyapatite in interaction with the buffered solution (HA-L/SBF+T/50; HA-L/SBF+T/100). After 7 days, the specific surface area increased to 1.4 and 1.7 $m^2 \cdot g^{-1}$, after 14 days the growth continued to 2.1 and 2.8 $m^2 \cdot g^{-1}$, and, after 21 days of steady growth, the specific surface area values increased to 4.0 and 4.6 $m^2 \cdot g^{-1}$, respectively.

At the end of the *in vitro* test, most of the tested porous granules showed a plateau (or a decrease) in the specific surface area values (59 - 65 $m^2 \cdot g^{-1}$). The percentage increase of the specific surface was nearly one order of magnitude higher for the sintered materials (HA-L samples) than for the highly porous ones (HA-H samples).

Weights of the tested synthetic materials

The percentage changes in the weight (Δm calculation showed in ref. [28]) of the sintered and porous hydroxyapatites after 7, 14 and 21 days of interaction with the two volumes of SBF and SBF+T solutions are shown in Table 4.

The trend in the changes in the weight of the sintered and porous hydroxyapatites is very similar to that of the change in the specific surface area values. Again, it was confirmed that, for most of the tested

Table 4. Weight changes (Δm) of **HA-L**, **HA-H** after 7, 14 and 21 days of interaction with **SBF** and **SBF+T**.

Type of material	Weight change Δm (%)		
	7 D	14 D	21 D
HA-L/SBF/50	0.6	1.0	0.8
HA-L/SBF/100	2.1	2.2	1.8
HA-L/SBF+T/50	2.0	3.7	3.3
HA-L/SBF+T/100	2.2	1.2	6.7
HA-H/SBF/50	15.6	19.8	20.8
HA-H/SBF/100	23.5	28.1	30.7
HA-H/SBF+T/50	14.9	18.3	18.7
HA-H/SBF+T/100	16.0	30.9	32.6

Table 3. Values and standard deviations of the specific surface area (Sa) of **HA-L**, **HA-H** before (0 day) and after (7, 14 and 21 days) interaction with **SBF** and **SBF+T**.

Type of material	Specific surface area S_a [$m^2 \cdot g^{-1}$]			
	0 D	7 D	14 D	21 D
HA-L/SBF/50	0.58 ± 0.10	2.42 ± 0.44	2.97 ± 0.38	2.23 ± 0.28
HA-L/SBF/100		2.51 ± 0.21	2.60 ± 0.32	1.60 ± 0.10
HA-L/SBF+T/50		1.74 ± 0.14	2.15 ± 0.06	4.03 ± 0.25
HA-L/SBF+T/100		1.37 ± 0.06	2.81 ± 0.44	4.56 ± 0.05
HA-H/SBF/50	49.39 ± 0.04	61.41 ± 0.07	61.46 ± 0.06	61.88 ± 0.06
HA-H/SBF/100		61.52 ± 0.08	60.11 ± 0.08	58.61 ± 0.06
HA-H/SBF+T/50		60.38 ± 0.11	62.52 ± 0.09	64.85 ± 0.11
HA-H/SBF+T/100		60.07 ± 0.11	54.25 ± 0.05	57.48 ± 0.08

samples, the most significant change occurred in the first 7 days of exposure to the solution. For the sintered hydroxyapatite, the change was from 0.6 to 2.2 % and, for the porous one, the change was from 15 to 23.5 %. Thereafter, the trend of the weight change slowed down or decreased, similarly as the specific surface. In the group of tested samples, the most reactive sample was the one interacting with the high volume of buffered solution (HA-L/SBF+T/100). The effect of the different solution volumes was visible in the second half of the experiment for the porous samples. In the case of 50 ml of the solution (HA-H/SBF/50; HA-H/SBF+T/50), the values were around 18 - 19 % after 14 days and around 19 - 20 % after 21 days. In the case of 100 ml of the solution (HA-H/SBF/100; HA-H/SBF+T/100), the values after 14 and 21 days were around 28 - 33 %. The increase in the weight for all types of samples indirectly indicates the precipitation of hydroxyapatite which is in agreement with the results of the solution analysis (Chapter "Analysis of the SBF and SBF+T leachates").

Surface morphology characterisation

Visual changes on the surface of the sintered hydroxyapatite with the low specific surface area (**HA-L**) before and after 7 and 14 days of interaction with the two volumes (50 and 100 ml) of **SBF** and **SBF+T** solutions are shown in Figure 1.

A comparison of images of the surfaces of the low surface area material (**HA-L**) before and after exposure to the solutions clearly shows their significantly different morphology. This implies that the different volumes of the solutions (50 and 100 ml) with and without the buffer (**SBF** and **SBF+T**) strongly contributed to the final structure of the precipitates formed on the surface of the tested material. The low-porous hydroxyapatite interacts immediately with the solution because as early as after 7 days a new phase of precipitated hydroxyapatite (HAp) is visible on all the surfaces, covering the entire surface of the tested granules. If the granules are exposed to 50 ml of SBF solution (Figure 1b) their surface is covered with globular precipitates of 2 - 5 µm in size, which are interconnected. After 14 days of exposure in the solution (Figure 1c), their size increased to 5 - 10 µm. When the

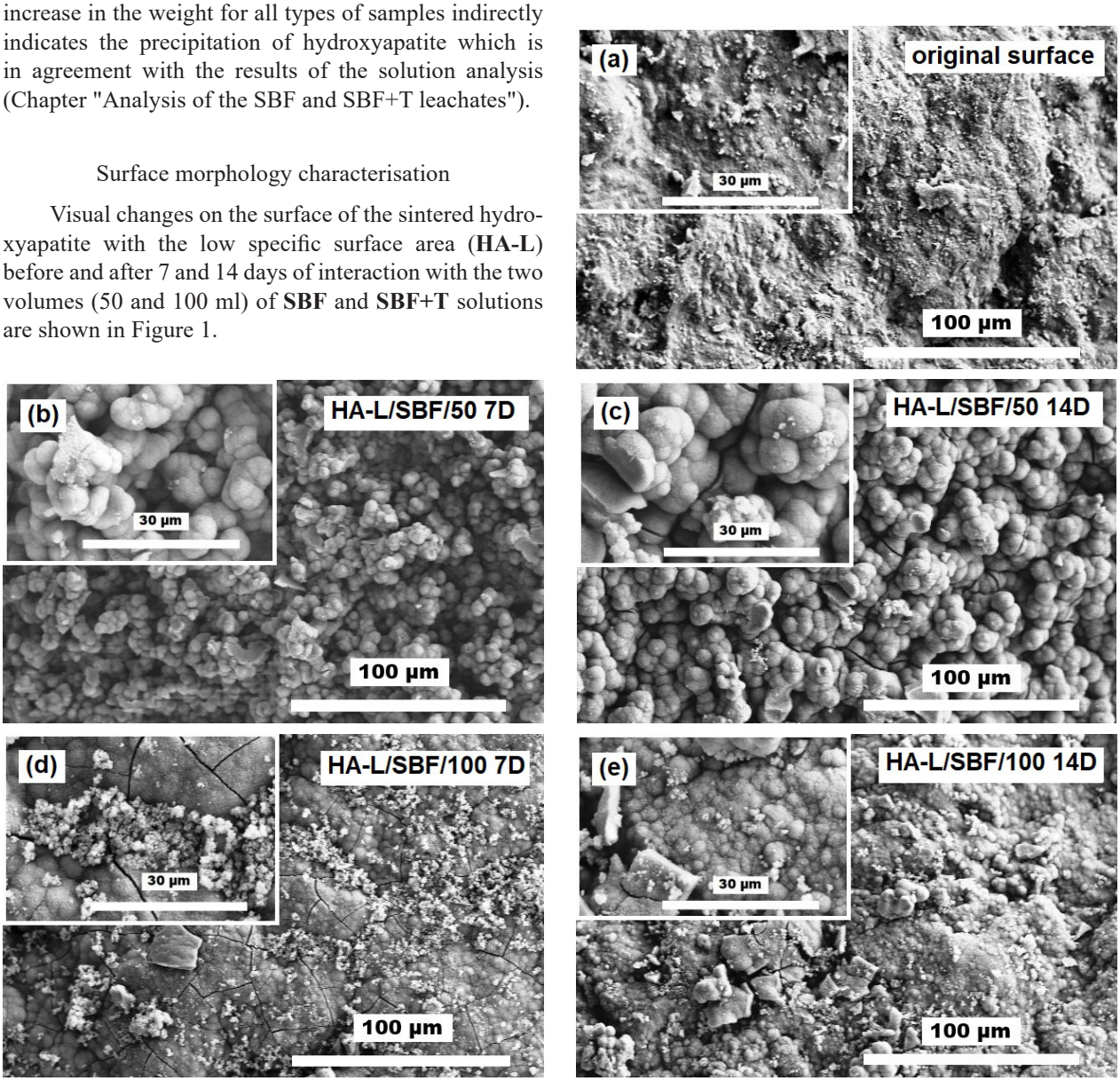

Figure 1. (SEM) Surface of HA-L: original surface a), HA-L/SBF/50 after 7 b) and after 14 c) days with SBF, HA-L/SBF/100 after 7 d) and after 14 e) days with SBF; HA-L/SBF+T/50 after 7 f) and after 14 g) days with SBF+T, HA-L/SBF+T/100 after 7 h) and after 14 i) days with SBF+T.

continues on next page ...

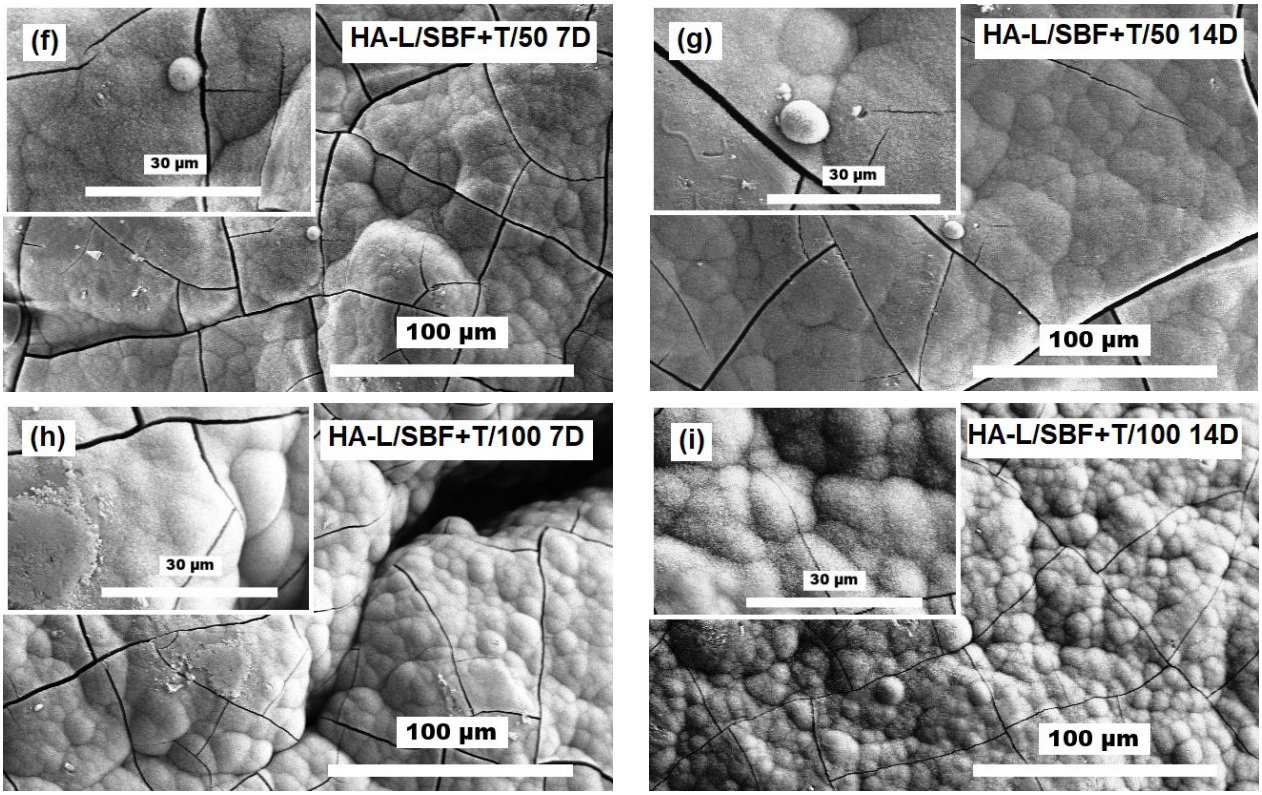

Figure 1. (SEM) Surface of HA-L: original surface a), HA-L/SBF/50 after 7 b) and after 14 c) days with SBF, HA-L/SBF/100 after 7 d) and after 14 e) days with SBF; HA-L/SBF+T/50 after 7 f) and after 14 g) days with SBF+T, HA-L/SBF+T/100 after 7 h) and after 14 i) days with SBF+T.

material was exposed to a larger volume (Figure 1d), after 7 days, the surface was completely covered with a thin layer of bone apatite composed of rosette-like nanocrystals. The thickness of the layer was about 10 - 15 µm after 14 days as can be clearly seen in the close-up image (Figure 1e). Precipitates of presumably amorphous white particles smaller than 1 µm are visible on this layer. A layer of precipitated hydroxyapatite that covered the granules of the test material exposed to the Tris-buffered solution after 7 days is visually quite different (Figure 1f). That layer is composed of plate-like nanocrystals clustered in globules so tightly arranged that they form a highly compact unit. The layer is significantly cracked after drying, but it does not peel off from the original material. After a 7-day exposure to a larger volume (100 ml) of the buffered solution, the same, dense layer of precipitated nanocrystalline hydroxyapatite (HAp) can be seen on the surface, but another layer is growing on top of it, as can be clearly seen in the close-up image (Figure 1h). The trend continued for the following 14 days, until the end of the 21-day *in vitro* experiment.

Visual changes on the surface of hydroxyapatite with the high specific surface area (**HA-H**) before and after 7 and 14 days of interaction with the two volumes of the **SBF** and **SBF+T** solutions are shown in Figure 2.

In the case of synthetic hydroxyapatite with the high specific surface area (HA-H), the surface changes are not as distinct at first sight as in the case of the material with the low specific surface area (HA-L). The surface of the original porous material prior to exposure (Figure 2a) has a very fine morphology that reacts with the solution under different conditions than the sintered material. After 7 days of exposure to both the buffered and unbuffered solutions the surface of the granules is covered with a thin layer of small crystals. After 14 days, the process of precipitation of the new phase continues

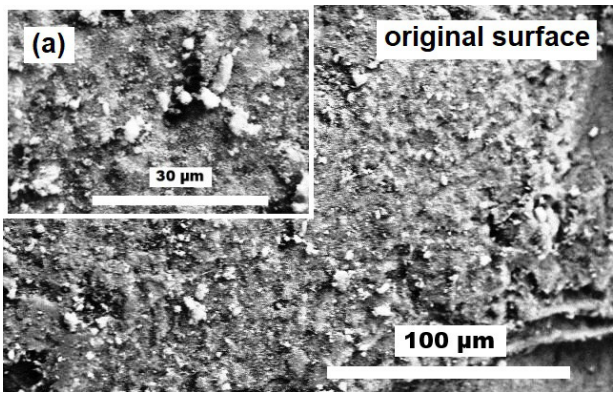

Figure 2. (SEM) Surface of HA-H: a) original surface after 7 days ...

continues on next page ...

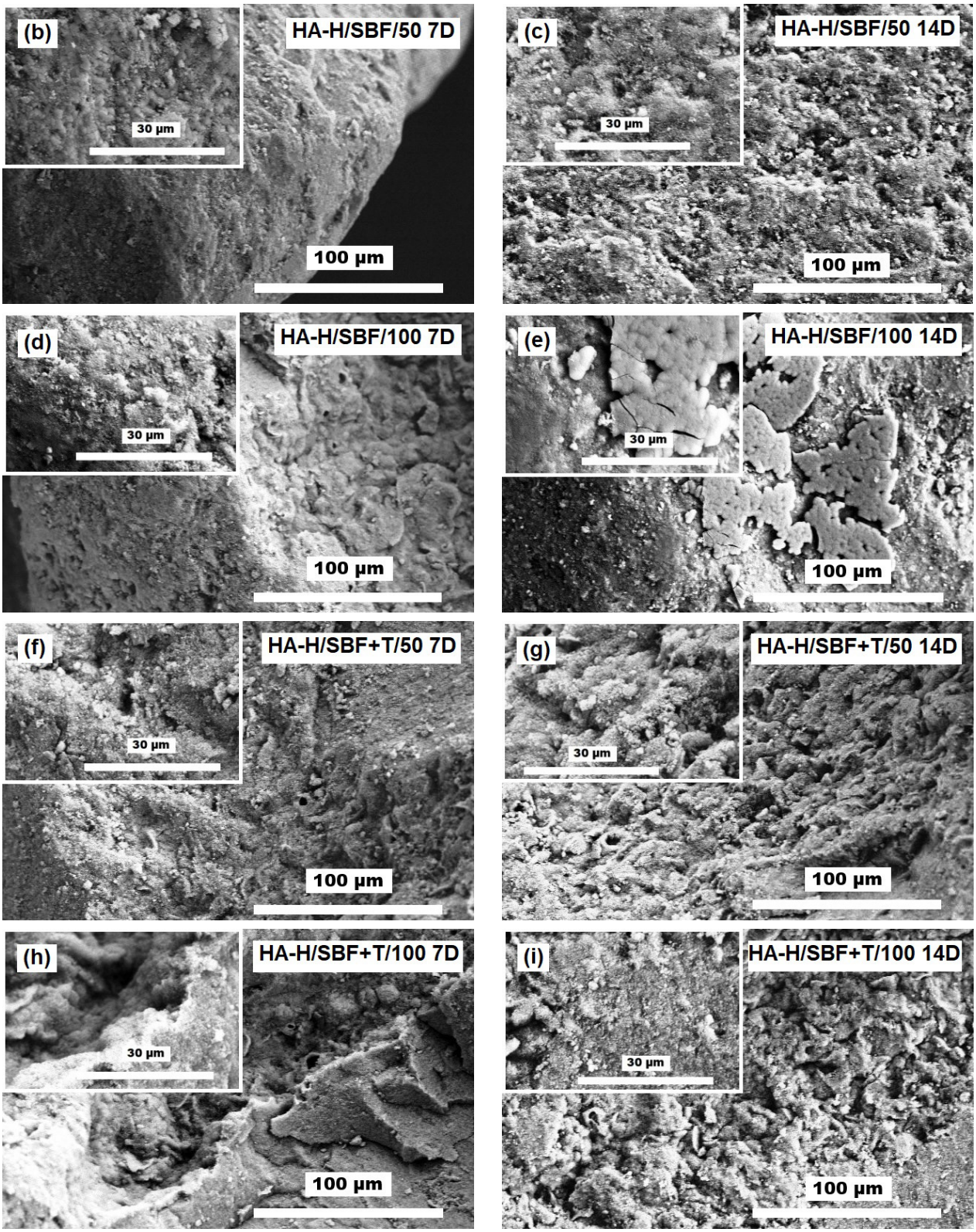

Figure 2. (SEM) Surface of HA-H: original surface a), HA-H/SBF/50 after 7 b) and after 14 c) days with SBF, HA-H/SBF/100 after 7 d) and after 14 e) days with SBF; HA-H/SBF+T/50 after 7 f) and after 14 g) days with SBF+T, HA-H/SBF+T/100 after 7 h) and after 14 i) days with SBF+T.

(as confirmed by the weight change) and this phase can be better seen in close-up images (Figure 2c). The exposure to a larger volume (100 ml) results in layering and the new phase formed by interconnected globules is clearly visible in the close-up image in Figure 2e. A thin layer of a new Ca-P phase perfectly reproduces the surface of the original material.

Analysis of the SBF and SBF+T leachates

Figure 3 shows the calcium ion concentrations in the **SBF** and **SBF+T** solutions during the interaction with the two types of HA material.

Figure 3a clearly shows a significant difference between the $(Ca)^{2+}$ ion concentrations in the **SBF+T** solution for the sintered and porous materials. Throughout the interaction, the ions are removed from the solution as all the measured values are below the original concentration (original **SBF+T**). The fastest decrease is observed for the material with the high specific surface area (**HA-H**) during the first 7 days of interaction. Then the rate slows down and stabilises from day 14 to the end of the experiment (40 - 50 $mg \cdot l^{-1}$). The smaller difference is also visible for the two different solution volumes. A greater calcium ion depletion is typical for the materials exposed to 50 ml of **SBF+T**. When comparing the concentration changes in the buffered and unbuffered solutions (Figure 3b), the effect of Tris buffer can be observed. The most pronounced effect of the buffer was observed for the sintered material (**HA-L**) where the value at the end of the experiment decreased from the initial 105 to about 40 $mg \cdot l^{-1}$, while, at the end of the experiment with the buffered **SBF+T** solution, it was about 95 $mg \cdot l^{-1}$.

Figure 4 shows the phosphate ion concentrations in the **SBF** and **SBF+T** solutions during the interaction with the high and low porous HA.

The changes in the phosphate ion concentrations in 50 and 100 ml of both types of solutions were very similar to those of the calcium ions, but the depletion was even more pronounced, especially for the porous surface. In the first 7 days of interaction, the process is the fastest, the most pronounced as it corresponds to the rapid precipitation of new phases on the surface of the tested granules (Figure 4a). After 14 days, the process slows down and, at the end of the in vitro test, the values stabilise. Again, there is a marked difference between the porous and sintered materials, with values at the end of the test ranging from 80 to 92 and 7 to 21 $mg \cdot l^{-1}$ respectively, compared to the initial value of 107 $mg \cdot l^{-1}$. The difference between the concentrations of the $(PO_4)^{3-}$ ions in 50 and 100 ml of the **SBF+T** solutions is again the same, about 10 %. A comparison between the buffered (Figure 4a) and unbuffered solutions (Figure 4b) shows the same trend as the calcium ions. The influence of the buffer is detected for the sintered material (**HA-L**) where, at the end of the interaction with the unbuffered SBF solution, the phosphate ion concentrations reached 4 - 6 $mg \cdot l^{-1}$ from the original 105 $mg \cdot l^{-1}$ (original **SBF**). The decrease in the calcium and phosphate ions in the

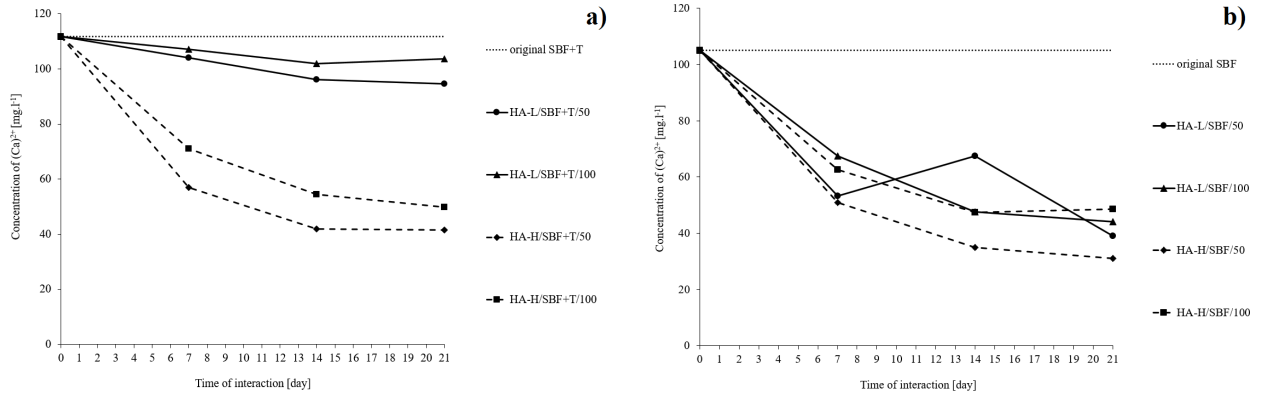

Figure 3. Concentration of the $(Ca)^{2+}$ ions in the: a) **SBF+T** and b) **SBF** solutions during the interaction with the bioceramic materials.

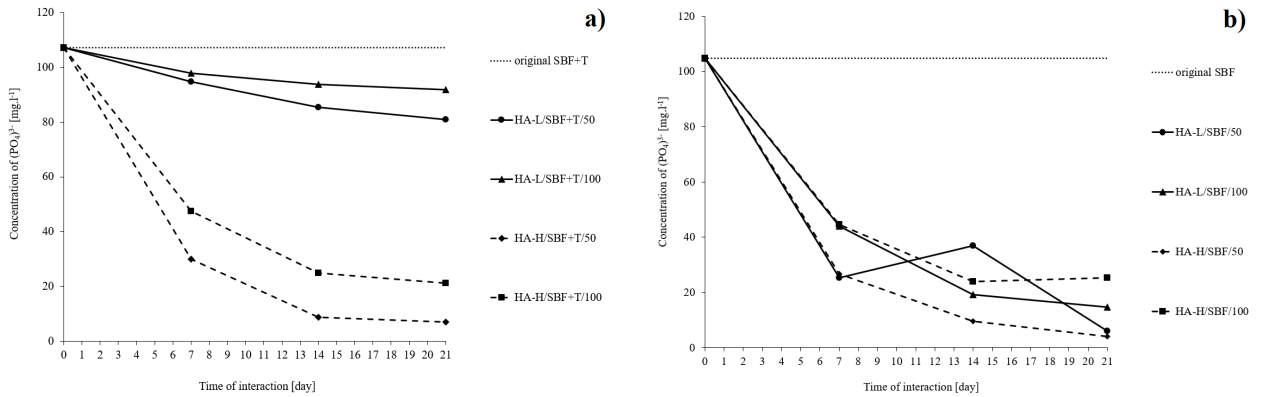

Figure 4. Concentration of the $(PO_4)^{3-}$ ions in the: a) **SBF+T** and b) **SBF** solutions during the interaction with the bioceramic materials.

solution (i.e., the kinetics of the calcium phosphate precipitation) is much more influenced by the specific surface of the samples in the buffered solutions than in the unbuffered ones (Figure 3a and 4a). In the unbuffered solutions, the kinetics is similar for all the samples and test conditions (Figure 3b and 4b).

Figure 5 shows the pH values in the **SBF** and **SBF+T** solutions during the interaction with the high and low porous synthetic HA.

The found changes in the calcium and phosphate ions concentrations in the **SBF** and **SBF+T** solutions are confirmed by the changes in the pH values in both types of solution (Figure 5a, b). The trends best demonstrate the influence of the **SBF+T** solution which maintained a stable pH throughout the in vitro assay (Figure 5a). For the sintered material, the change was only slightly higher at 7.5 compared to the porous material, where the measured value was 7.4. The difference between the solution volumes (50 and 100 ml) was also minimal for the buffered solution. However, in the unbuffered the material, precipitated under all the conditions used. This was expected when testing commercial granules of synthetic hydroxyapatite. However, it is obvious that the morphology, size, density and thickness of the layer vary under different test conditions and they are also influenced by the surface of the material. The analyses of the solutions positively confirmed the dramatically different rates of ion removal, which was most pronounced during the first 7 days. The pH analyses of the buffered and unbuffered solutions clearly detected the influence of the Tris buffer. The development of new ceramics or glass-based fragmented biomaterials (granules, crumbs, powders), therefore, poses questions as to which *in vitro* test conditions should be used to predict their bioactive properties. It is necessary to select such test conditions, i.e., combinations of the material, solution, weight of the tested material, its porosity, surface area, volume of the solution and solution replacement or flow, which will not affect the results in a positive or negative manner.

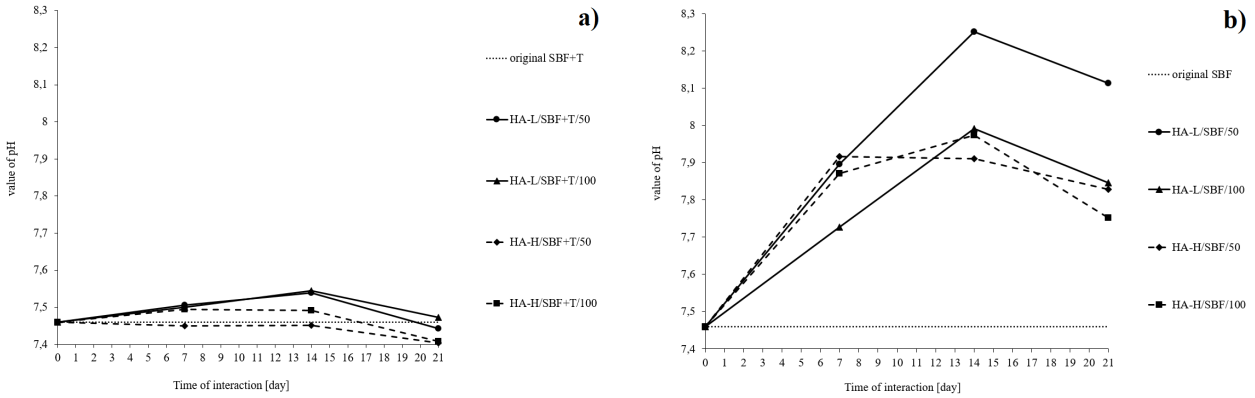

Figure 5. Values of the pH in the: a) **SBF+T** and b) **SBF** solutions during the interaction with the bioceramic materials.

SBF solution, a significant change from the original value (7.4) occurred in all the cases and all the volumes, most notably in the first 7 to 14 days of interaction, up to around 7.9 to 8.2. Thereafter, the pH decreased and, at the end of the experiment, the values slow down to 7.5 to 8. The sintered material (**HA-L**) responded most sensitively to both the buffered and unbuffered solutions, as the values were around 7.4 - 7.5 in the case of **SBF+T** and around 7.9 - 8 in the case of **SBF**.

CONCLUSIONS

The purpose of this paper was not to criticise the standard or to strictly identify properties of the tested commercial bioceramic materials. The commercial material was chosen due to the good possibility of its analysis in comparison with newly developed materials. The *in vitro* test conditions were proposed rather to reflect on how they may influence the results. The bone hydroxyapatite (HAp), which is a sign of bioactivity of

REFERENCES

1. Best S. M., Porter A. E., Thian E. S., Huang J. (2008): Bioceramics: Past, present and for the future. *Journal of the European Ceramic Society, 28*(7), 1319-1327. doi:10.1016/j.jeurceramsoc.2007.12.001
2. Cao W., Hench L. L. (1996): Bioactive materials. *Ceramics international, 22*(6), 493-507.doi:10.1016/0272-8842(95)00126-3
3. Pena J., Vallet-Regı M. (2003): Hydroxyapatite, tricalcium phosphate and biphasic materials prepared by a liquid mix technique. *Journal of the European Ceramic Society, 23*(10), 1687-1696.doi:10.1016/S0955-2219(02)00369-2
4. Xu J. L., Khor K. A., Dong Z. L., Gu Y. W., Kumar R., Cheang P. (2004): Preparation and characterization of nano-sized hydroxyapatite powders produced in a radio frequency (rf) thermal plasma. *Materials Science and Engineering: A, 374*(1-2), 101-108. doi:10.1016/j.msea.2003.12.040
5. Feng W., Mu-Sen L., Yu-Peng L., Yong-Xin Q. (2005): A simple sol–gel technique for preparing hydroxyapatite nanopowders. *Materials Letters, 59*(8-9), 916-919.doi:10.1016/j.matlet.2004.08.041

6. Fathi M. H., Hanifi A. (2007): Evaluation and characterization of nanostructure hydroxyapatite powder prepared by simple sol–gel method. *Materials letters, 61*(18), 3978-3983.doi: 10.1016/j.matlet.2007.01.028
7. Fathi M. H., Hanifi A., Mortazavi V. (2008): Preparation and bioactivity evaluation of bone-like hydroxyapatite nanopowder. *Journal of materials processing technology, 202*(1-3), 536-542.doi:10.1016/j.jmatprotec.2007.10.004
8. Uehira M., Okada M., Takeda S., Matsumoto N. (2013): Preparation and characterization of low-crystallized hydroxyapatite nanoporous plates and granules. *Applied surface science, 287*, 195-202.doi:10.1016/j.apsusc.2013.09.117
9. Grigoraviciute-Puroniene I., Tanaka Y., Vegelyte V., Nishimoto Y., Ishikawa K., Kareiva A. (2019): A novel synthetic approach to low-crystallinity calcium deficient hydroxyapatite. *Ceramics International, 45*(12), 15620-15623. doi:10.1016/j.ceramint.2019.05.072
10. Kalpana M., Nagalakshmi R. (2023): Effect of reaction temperature and pH on structural and morphological properties of hydroxyapatite from precipitation method. J*ournal of the Indian Chemical Society, 100*(4), 100947. doi:10.1016/j.jics.2023.100947
11. Ooi C. Y., Hamdi M., Ramesh S. (2007): Properties of hydroxyapatite produced by annealing of bovine bone. *Ceramics international, 33*(7), 1171-1177.doi:10.1016/j.ceramint.2006.04.001
12. Ruksudjarit A., Pengpat K., Rujijanagul G., Tunkasiri T. (2008): Synthesis and characterization of nanocrystalline hydroxyapatite from natural bovine bone. *Current applied physics, 8*(3-4), 270-272.doi:10.1016/j.cap.2007.10.076
13. Arokiasamy P., Abdullah M. M. A. B., Abd Rahim S. Z., Luhar S., Sandu A. V., Jamil N. H., Nabiałek M. (2022): Synthesis methods of hydroxyapatite from natural sources: A review. *Ceramics International, 48*(11), 14959-14979. doi:10.1016/j.ceramint.2022.03.064
14. Yadav M. K., Shukla R. H., Prashanth K. G. (2023): A comprehensive review on development of waste derived hydroxyapatite (HAp) for tissue engineering application. *Materials Today: Proceedings,* in press. doi:10.1016/j.matpr.2023.04.669
15. Kolmas J., Krukowski S., Laskus A., Jurkitewicz M. (2016): Synthetic hydroxyapatite in pharmaceutical applications. *Ceramics International, 42*(2), 2472-2487.doi:10.1016/j.ceramint.2015.10.048
16. Stanić V., Dimitrijević S., Antić-Stanković J., Mitrić M., Jokić B., Plećaš I. B., Raičević S. (2010): Synthesis, characterization and antimicrobial activity of copper and zinc-doped hydroxyapatite nanopowders. *Applied Surface Science, 256*(20), 6083-6089.doi:10.1016/j.apsusc.2010.03.124
17. Nenen A., Maureira M., Neira M., Orellana S. L., Covarrubias C., Moreno-Villoslada I. (2022): Synthesis of antibacterial silver and zinc doped nano-hydroxyapatite with potential in bone tissue engineering applications. *Ceramics International, 48*(23), 34750-34759.doi:10.1016/j.ceramint.2022.08.064
18. Coelho C. C., Araújo R., Quadros P. A., Sousa S. R., Monteiro F. J. (2019): Antibacterial bone substitute of hydroxyapatite and magnesium oxide to prevent dental and orthopaedic infections. *Materials Science and Engineering: C, 97*, 529-538.doi:10.1016/j.msec.2018.12.059
19. Kim H. J., Kwon T. Y., Son J. S. (2018): Fabrication and *in vitro* evaluation of natural duck beak bone/synthetic hydroxyapatite bi-layered scaffold for bone regeneration. *Materials Letters, 220*, 186-189.doi: 10.1016/j.matlet.2018.03.017
20. Kubasiewicz-Ross P., Hadzik J., Seeliger J., Kozak K., Jurczyszyn K., Gerber, H., et al. (2017): New nano-hydroxyapatite in bone defect regeneration: A histological study in rats. *Annals of Anatomy-Anatomischer Anzeiger, 213*, 83-90.doi:10.1016/j.aanat.2017.05.010
21. Kokubo T., Takadama H. (2006): How useful is SBF in predicting *in viv*o bone bioactivity?. *Biomaterials, 27*(15), 2907-2915.doi:10.1016/j.biomaterials.2006.01.017
22. Sánchez-Salcedo S., Balas F., Izquierdo-Barba I., Vallet-Regí M. (2009): In vitro structural changes in porous HA/β-TCP scaffolds in simulated body fluid. *Acta Biomaterialia, 5*(7), 2738-2751. doi:10.1016/j.actbio.2009.03.025
23. Bohner M., Lemaitre J. (2009): Can bioactivity be tested in vitro with SBF solution?. *Biomaterials, 30*(12), 2175-2179. doi:10.1016/j.biomaterials.2009.01.008
24. ISO 23317:2014 Implants for surgery - In vitro evaluation for apatite-forming ability of implant materials; Geneva, 2014.
25. Sroka-Bartnicka A., Borkowski L., Ginalska G., Ślósarczyk A., Kazarian S. G. (2017): Structural transformation of synthetic hydroxyapatite under simulated in vivo conditions studied with ATR-FTIR spectroscopic imaging. *Spectrochimica Acta Part A: Molecular and Biomolecular Spectroscopy, 171*, 155-161.doi:10.1016/j.saa.2016.07.051
26. Leng Y., Chen J., Qu S. (2003): TEM study of calcium phosphate precipitation on HA/TCP ceramics. *Biomaterials, 24*(13), 2125-2131.doi:10.1016/S0142-9612(03)00036-X
27. Horkavcova D., Zitkova K., Rohanova D., Helebrant A., Cilova Z. (2010). The Resorption of ß-TCP and HA materials under conditions similar to those in living organisms. *Ceramics-Silikáty, 54*, 398-404.
28. Horkavcova D., Rohanova D., Kuncova L., Zitkova K., Cilova Z. Z., Helebrant A. (2014): Comparison of reactivity of synthetic and bovine hydroxyapatite in vitro under dynamic conditions. *Ceramics-Silikáty, 58*(1), 70-78.
29. Rohanová D., Horkavcová D., Helebrant A., Boccaccini A. R. (2016): Assessment of in vitro testing approaches for bioactive inorganic materials. *Journal of Non-Crystalline Solids, 432*, 53-59.doi:10.1016/j.jnoncrysol.2015.03.016
30. Horkavcová D., Stříbny A., Schuhladen K., Bezdička P., Boccaccini A. R., Rohanová D. (2021): Effect of buffer in simulated body fluid on morphology and crystallinity of hydroxyapatite precipitated on 45S5 bioactive glass-derived glass–ceramic scaffolds: comparison of Good's buffer systems and TRIS. *Materials Today Chemistry, 21*, 100527. doi:10.1016/j.mtchem.2021.100527